Theor Appl Climatol (2014) 115:355–364
DOI 10.1007/s00704-013-0998-6

ORIGINAL PAPER

Influence of non-feedback variations of radiation on the determination of climate feedback

Yong-Sang Choi · Heeje Cho · Chang-Hoi Ho · Richard S. Lindzen · Seon Ki Park · Xing Yu

Received: 9 January 2013 / Accepted: 13 August 2013 / Published online: 5 September 2013

Abstract Recent studies have estimated the magnitude of climate feedback based on the correlation between time variations in outgoing radiation flux and sea surface temperature (SST). This study investigates the influence of the natural non-feedback variation (noise) of the flux occurring independently of SST on the determination of climate feedback. The observed global monthly radiation flux is used from the Clouds and the Earth's Radiant Energy System (CERES) for the period 2000–2008. In the observations, the time lag correlation of radiation and SST shows a distorted curve with low statistical significance for shortwave radiation while a significant maximum at zero lag for longwave radiation over the tropics. This observational feature is explained by simulations with an idealized energy balance model where we see that the non-feedback variation plays the most significant role in distorting the curve in the lagged correlation graph, thus obscuring the exact value of climate feedback. We also demonstrate that the climate feedback from the tropical longwave radiation in the CERES data is not significantly affected by the noise. We further estimate the standard deviation of radiative forcings (mainly from the noise) relative to that of the non-radiative forcings, i.e., the noise level from the observations and atmosphere–ocean coupled climate model simulations in the framework of the simple model. The estimated noise levels in both CERES (>13 %) and climate models (11–28 %) are found to be far above the critical level (~5 %) that begins to misrepresent climate feedback.

Y.-S. Choi (✉) · S. K. Park
Department of Environmental Science and Engineering, Ewha Womans University, Daehyeon-dong, Seodaemun-gu, Seoul 120-750, Korea
e-mail: ysc@ewha.ac.kr

H. Cho · C.-H. Ho
Computational Science and Technology, Seoul National University, Seoul, Korea

C.-H. Ho
School of Earth and Environmental Sciences, Seoul National University, Seoul, Korea

R. S. Lindzen
Department of Earth, Atmospheric and Planetary Sciences, Massachusetts Institute of Technology, Cambridge, Massachusetts, USA

X. Yu
Tropical Marine Science Institute, National University of Singapore, Singapore, Singapore

1 Introduction

Because the only direct global energy measurements are from satellites, recent studies have attempted to determine climate feedback from satellite retrievals (Forster and Gregory 2006; Lindzen and Choi 2009, 2011; Spencer and Braswell 2010, 2011). The previous results, however, have shown acute contradiction between the likelihood of positive and negative climate feedbacks. High total positive climate feedback brings in fundamentally more uncertainties in climate sensitivity than negative climate feedback does (Roe and Baker 2007; Lindzen and Choi 2011). Thus, currently, the huge error range of the estimated magnitude of high climate sensitivity includes all of the values found in current climate models that represent total positive climate feedback (Colman 2003; Soden and Held 2006; Knutti and Hegerl 2008).

Climate feedback processes essentially yield the change in outgoing radiation flux in response to the change in global surface temperature through the changes of cloud, water vapor, etc. Thus, the recent observational feedback studies were based mostly on simple linear regression between global

surface temperature anomalies (ΔT_s) and the flux anomalies of global net radiation (ΔR, sum of shortwave and longwave radiation flux anomalies). The basis of examining the relation between ΔR and ΔT_s to estimate a feedback strength is that radiative flux is controlled by temperature over a given time in feedback. Most theoretical and empirical experiments showed that the exact value of feedback appears as the regression slope $\Delta R/\Delta T_s$ at zero time lag when the feedback between the two variables dominates over the system (Frankignoul et al. 1998; Frankignoul 1999). More importantly, this should be followed by significant correlation at zero lag. The total climate feedbacks estimated by this way were usually positive.

However, recent observations show that correlation between ΔR and ΔT_s at zero lag is very weak and moreover is often located between the opposite signs at negative and positive month lags (Lindzen and Choi 2011). The weak correlation between the two variables implied that in observations, many unknown radiative processes that are not feedbacks to sea surface temperature (SST) (e.g., random cloud variations) exist and that they strongly confuse the feedback strength in the ΔR–ΔT_s relation. This may also be the case of feedbacks taking several weeks to fully develop, e.g., cirrus detrainment from tropical cumulonimbus. However, as assumed in most of previous feedback studies, this study rules out such a delayed feedback process. This naturally casts a question about the reliability of the feedback estimates from the zero lag simple regression of observational time series.

In order to resolve the problems associated with the simple regression method, improved methods have been suggested by Lindzen and Choi (2009, 2011) and Spencer and Braswell (2010). All these studies have argued the likelihood of negative feedback by applying different methods that may better isolate the feedbacks from the effects of continuous equilibration or long-term (i.e., several decades) trend. Lindzen and Choi (2009, 2011) used short (few-month) segments in which the increase (or decrease) in ΔR and ΔT_s occurred. Spencer and Braswell (2010) tracked sequential ΔR and ΔT_s and found that feedback processes are presented by thin stripes in the ΔR–ΔT_s chart. Both methods aim to isolate feedbacks from the confounding factors of equilibration or long-term trend more appropriately than does the simple regression of the whole observed time series. However, these alternatives have also been subject to criticism (Chung et al. 2010; Murphy 2010; Trenberth et al. 2010).

Of course, uncertainties in the previous feedback estimates were acknowledged (Spencer and Braswell 2011), but the reason for the uncertainties remains unclear. Not knowing clearly the reason prevents the improved determination of the feedback strength. As we show here, the main reason turns out to be a significant influence of natural variations of radiation that are not related to feedback processes (called "non-feedback" variations or noise in this study). They are in fact hardly isolated from the observed flux anomalies ΔR in which both feedback and non-feedback variations are blended, even by many currently known methods (including two alternative methods by Spencer and Braswell 2010 and Lindzen and Choi 2011).

In order to avoid spurious contribution of the non-feedback variations to feedback, the use of a "lagged covariance" has been suggested (Frankignoul et al. 1998; Frankignoul 1999). This is because the cause and effect of the change in outgoing radiation fluxes can be identified from lagged covariances. However, only in the case when ΔT_s is mostly remotely generated in time is it likely that the atmospheric response can reflect the true atmospheric feedback in the stochastic determination (Frankignoul 1999). We shall begin the discussion on the influence of non-feedback variations, with the lagged correlation analysis between observed sequential ΔR and ΔT_s.

2 Cross-correlation results between radiation flux and SST

We obtained the radiation flux data from the Clouds and the Earth's Radiant Energy System (CERES) single scanner footprint (SSF, version 2.6, Wielicki et al. 1998) onboard the Terra satellite. The flux data were correlated with the SST from the NOAA (OISST, version 2). Here, we used SST instead of global surface temperature because land surface temperature is highly variable in observations, providing large uncertainty in determination of climate feedbacks. The analysis period is from March 2000 to June 2011 (136 months); the time and spatial resolutions are monthly and 1°, respectively. Both data were then deseasonalized by monthly climatological means to produce the anomalies of global (both land and ocean) outgoing fluxes and SST, ΔR, and ΔT_s. Then the (lagged) cross-correlation analysis is applied to the two anomalies; the correlations and the regression slopes are shown in Fig. 1a, b, respectively.

The cross-correlation results with respect to time lag are shown for longwave (LW, red line) and shortwave (SW, blue line) radiation fluxes (Fig. 1a). The thick solid line indicates global average, and the thick dashed line indicates tropical average (20°S–20°N). Negative lags indicate that ΔR precedes ΔT_s, whereas positive lags indicate that ΔT_s precedes ΔR. The reason for using ΔT_s as the abscissa is because feedbacks are usually defined and reckoned with respect to changes in surface temperature. As a whole, fairly variable correlation coefficients (r) are found according to time lags. Interestingly, only LW in the tropics (20°S–20°N) shows a distinctively highest correlation at zero lag (thick dashed red line in Fig. 1a).

At the approximate emission temperature of the earth of 255 K and assuming that the emission temperature is linearly related with the surface temperature, the effective Planck longwave cooling is known to be 3.3 W m^{-2} K^{-1} for small

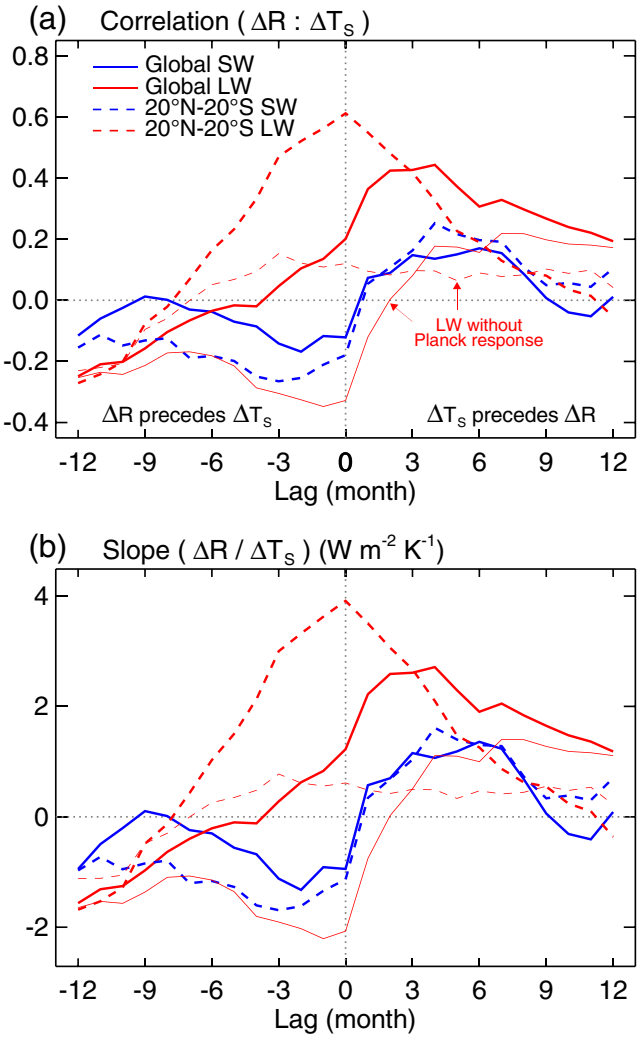

Fig. 1 The lagged linear correlation coefficient (**a**) and regression slope (**b**) of ΔR versus ΔT_s for shortwave (*blue*) and longwave (*red*) radiation; the *thick solid line* indicates global data, and the *thick dashed line* indicates 20°S–20°N. The *thin red line* indicates longwave radiation where Planck response is excluded. In the paper, positive signs are used for upward fluxes

perturbations of the surface temperature (e.g., Trenberth et al. 2010; Lin et al. 2011; Lindzen and Choi 2011). This is the so-called Planck response that is proportional to SST and exclusion of which from LW flux is displayed by thin lines in Fig. 1a, b. Characteristically, in Fig. 1a, in LW where Planck response is excluded (thin red lines), the sign of correlation around zero lag is very different from LW where Planck response is originally included (thick red lines). Especially for the tropics, when Planck response was excluded from the LW flux anomalies, the convex-shaped correlation (i.e., a maximum at zero lag and lower values at non-zero lags) disappeared (compare thick and thin dashed red lines). This represents that the Planck response plays a crucial role in stabilizing the lagged correlation to have a highest value at zero lag. However, it should be noted that for obtaining LW climate feedback associated with specific variables like water vapor or clouds, exclusion of Planck response from LW flux is methodologically unavoidable.

We see from the distorted (usually S-shaped) correlation curves in Fig. 1a that the negative correlation at zero lag actually comes from ΔR preceding ΔT_s (i.e., negative lag) and that the correlation changes from negative to positive as ΔR follows ΔT_s (i.e., positive lag). This pattern is also very similar to the regression $\Delta R/\Delta T_s$ slopes in Fig. 1b. Eventually, this opposite sign clearly limits the statistical significance of regression slopes at zero lag, although the regression slope is highly fluctuating in the range of −2 to 4 W m^{-2} K^{-1} (Fig. 1b). For example, the coefficient of determination r^2 is only 2 % at zero lag for globally averaged SW flux (blue solid line in Fig. 1a); the corresponding $\Delta R/\Delta T_s$ value to this (approximately −1 W m^{-2} K^{-1} in Fig. 1b) is indeed too uncertain to represent a general feature of nature, or even to test climate models with the estimated climate feedback from the observation, given that model climate sensitivity is so sensitive to small uncertainty in climate feedbacks (Roe and Baker 2007). This weak significance at zero lag indicates that the estimation of SW feedback is essentially more difficult than LW feedback.

Fig. 1 also clearly compares global averages and tropical averages. The distortion seems more intensified for global averages than tropical averages. The tropical LW data excluding Planck response (thin dashed red lines in Fig. 1a, b) was much more convexly shaped than the global LW data excluding Planck response (thin solid red lines in Fig. 1a, b). These results imply that the estimation of global feedback is more difficult than tropical feedback. This is probably associated with major factors inducing ΔR that are mostly the non-feedback cloud changes commonly found to be more frequent in the extratropics and over land.

3 Distinguishing feedback from non-feedback noise

Clouds are the most important factors inducing large fluctuations of outgoing radiation. Clouds are associated with various weather phenomena such as fronts, convective system, topographic lee waves, etc. For them to form and dissipate, physical factors such as condensation aerosols, ambient humidity, etc. are very influential too. Hence, clouds depend on many factors other than surface temperature. Only the dependence on surface temperature T_s, however, is directly relevant to cloud feedback. We shall refer to the other factors as “noise” for the sake of distinguishing them from the feedback ‘signal’ in the outgoing radiation flux, though these factors are often more important to cloud formation and composition (note that optical properties of clouds can change—not just the cloud amount, Choi et al. 2010). The noise is also called effective radiative forcing elsewhere, defined as all the instantaneous radiative forcing including fast atmospheric adjustments occurring independently of T_s

(Gregory and Webb 2008). To be clear, the atmospheric factors like water vapor and temperature profiles are directly changed by ΔT_s, and in turn, indirectly changing clouds are not noise but are the feedback processes. Note that these too have already been included in our ΔR–ΔT_s analyses.

A key issue here is that the factors occurring independently of T_s (i.e., noise) must be excluded in the estimation of feedback from the ΔR–ΔT_s analysis. This is because doing otherwise generally leads to the distorted lagged correlation with low statistical significance (see Fig. 1). How this noise effect actually works on distorting the correlation is explained in the following. Based on our analysis, separating LW and SW, the total ΔR directly observed from the CERES is much more strongly correlated with SW anomalies (coefficient of determination, r^2=~60 %) than LW anomalies (r^2=~30 %), so it is likely that the total ΔR is primarily associated with SW radiation. Simply focusing on SW, for example, instantaneously increased cloud (independently of ΔT_s) would reflect more sunlight (positive ΔR) and thereby cool the surface (negative ΔT_s), which of necessity is a non-feedback contribution to ΔR. This case leads, of course, to negative $\Delta R/\Delta T_s$, overestimating positive cloud feedback from the ΔR–ΔT_s analysis.

In order to distinguish such spurious contributions to feedback from actual feedbacks, it is necessary to distinguish changes in ΔR that lead changes in ΔT_s (shown as negative lags) from those that lag (shown as positive lags). Only the latter should be considered to be feedbacks. To confirm the necessity of the lagged covariances in the present climate feedback problem, we run an idealized energy balance model assuming a hypothetical climate system with uniform temperature and heat capacity (Manabe et al. 1990; Schwartz 2007; Lin et al. 2011; Spencer and Braswell 2010). Though the model is too simple to simulate the earth's true climate, this model contains enough of the essential nature of climate to determine if the estimation of feedbacks is methodologically appropriate. The nature of climate in the model can be inferred from the known magnitudes and the time scales of climate responses to forcings, without reference to the detailed physical processes that are implemented in complex climate models. The simple model focuses just on the relationship of time series of ΔT_s and ΔR, which is essential for the estimation of feedbacks. By keeping simplicity at the cost of quantitative accuracy, the following simple model provides useful insight without the difficulties associated with complex climate models.

$$C_p\left[\frac{d\Delta T_s}{dt}\right] = F_{non}(t) + F_{rad}(t) - \lambda\cdot\Delta T_s(t) \tag{1}$$

where C_p is the constant bulk heat capacity of the system and λ is the parameter indicating the feedback strength. C_p determines the overall variance of surface temperature in response to a given amount of forcing and feedback. Here, C_p was set to 14 year W m^{-2} K^{-1} equivalent to 110 m of ocean water corresponding roughly to the ocean mixed layer (Schwartz 2007). Following Spencer and Braswell (2010) and Lindzen and Choi (2011), forcings in Eq. 1 are divided into two terms: radiative (F_{rad}) and non-radiative (F_{non}) forcings. F_{rad} can be due for example to cloud variations, while F_{non} may be due for example to stochastic component of heat transfer from ocean below the mixed layer. We did not consider the increasing radiative forcing such as due to increasing CO_2 that is known to cause other problems in estimating climate feedback (Spencer and Braswell 2010; also see Section 5 for more details). Two forcing terms (F_{rad} and F_{non}) are 9-month low pass-filtered series of monthly normally distributed random numbers with nearly zero mean, to mimic the time scales of variations seen in the climate models and observations (Spencer and Braswell 2011). F_{rad} may partly include forcings by cloud variations that are dynamically driven by F_{non}. Even in that case where F_{rad} and F_{non} are strongly correlated, F_{rad} remains to act as a noise source unless the cloud variations are involved in λ. $\lambda\Delta T_s$ represents radiative feedback effect. λ must have a positive value; otherwise, the system is unstable. The larger λ is, the faster the system is restored to equilibrium. Let λ_0 be the Planck response of 3.3 W m^{-2} K^{-1}, and then λ values larger (smaller) than λ_0 indicate negative (positive) feedbacks. In order to show that climate feedback can easily be estimated as being positive despite the true feedback being negative, we assumed the idealized system to have (negative) climate feedback 2.7 W m^{-2} K^{-1}, so λ in Eq. 1 is set to 6 (=2.7+3.3) W m^{-2} K^{-1}.

With monthly varying F and constant C_p and λ, it is now possible to simulate time series of temperature anomaly, ΔT_s from Eq. 1. We carried out finite difference integrations of Eq. 1 for 10 years on monthly time scale (Choi and Song 2012). The radiative forcing plus the feedback process in our model runs appears as the total outgoing radiative flux at the top of the atmosphere ΔR_{TOA}. To correspond to what the CERES instrument actually measures, instrumental or sampling errors (ε) should also be included in ΔR_{TOA}:

$$\Delta R_{TOA} = -F_{rad}(t) + \lambda\cdot\Delta T_s(t) + \varepsilon \tag{2a}$$

Subtracting the Planck response to surface temperature ($\lambda_0\Delta T_s$) from ΔR_{TOA}, the residual finally indicates outgoing flux anomaly without the Planck response as shown in Fig. 1.

$$\begin{aligned}\Delta R = \Delta R_{TOA} - \lambda_0\cdot\Delta T_s(t) &= -F_{rad}(t) \\ &\quad + \lambda\cdot\Delta T_s(t) - \lambda_0\cdot\Delta T_s(t) \\ &\quad + \varepsilon\end{aligned} \tag{2b}$$

It is widely accepted that ΔR is largely associated with cloud variation. However, the extraction of cloud-associated radiation introduces many other problems beyond those

considered here. In order to extract cloud forcing from TOA fluxes, one may use information from analyzed data obtained from sophisticated 3-D climate models. Such models are already influenced by the model treatment of clouds which is generally held to be unreliable. The present paper does not attempt to extract cloud forcing. Rather, we will use the radiation flux ΔR that is just the total outgoing radiation in which only the Planck response is removed to focus on feedbacks. Moreover, the present paper restricts itself to only the methodological problems associated with the use of simple regression.

We now inquire how the ΔR–ΔT_s lagged correlation is changed by noise. As explained above, both forcings (F_{non} and F_{rad}) in Eq. 1 are basically randomly generated Gaussian numbers with nearly zero mean, but their standard deviations are changed depending on the experiments in Figs. 2 and 3. Fig. 2a shows ΔR–ΔT_s correlations with respect to the lagged month of ΔR behind ΔT_s (the abscissa). The blue-shaded area is the range of the 1,000 repeated results by the simple model (10 years for each run), and the lines are 30 randomly selected examples. In Fig. 2a, we neglected the non-radiative forcing F_{non}, assuming that all the climatic forcing is purely radiative (observed at TOA) (i.e., $F_{non}=0$ and $F_{rad}\neq 0$); thus, T_s is changed by noise (like cooling effects of randomly-formed clouds) as well as the feedback process. Randomly generated Gaussian noise is in F_{rad}. The standard deviation of the forcing $\sigma(F_{rad})$ is set to 1 W m^{-2}. As we will estimate from observations in the next section, the present setting of $\sigma(F_{non})$ turns out to be quite reasonable. In these extensive runs in Fig. 2a, the maxima and minima of correlation coefficients (and regression slopes) were present within finite lead and lag months for most simulations. The detailed shape of the curve varies with randomly generated forcing, but the S-shaped curve is the most common if the forcing is purely radiative.

On the contrary, if the forcing is purely non-radiative (i.e., $F_{rad}=0$ and $F_{non}\neq 0$), most of the results of lagged analyses are similar to Fig. 2b. The standard deviation of the forcing $\sigma(F_{non})$ is set to 5 W m^{-2}. At larger or smaller lags, correlations are more variable and lower. Correlation was highest and constant at zero lag, resulting in that maxima of regression slopes at zero lag (i.e., the simultaneous regression) is the same as the true feedback 2.7 W m^{-2} K^{-1}. Results in Fig. 2a, b are completely different. Note that this difference stems from the fact that ΔR_{TOA} in the case of Fig. 2b is determined mainly by feedback processes ($\lambda\Delta T_s$), whereas ΔR_{TOA} in the case of Fig. 2a is determined by both feedback processes and radiative forcing ($-F_{rad}+\lambda\Delta T_s$) (see Eq. 2a).

In more realistic conditions that both F_{non} and F_{rad} are contributing as climatic forcings (Fig. 3), the characteristics of ΔR–ΔT_s correlation should be in between the two extreme cases (Fig. 2a, b). Fig. 3 shows examples of the lagged correlation (and regression slope) results for various $\sigma(F_{rad})/\sigma(F_{non})$=0.05 (a), 0.14 (b), and 2.33 (c); these are the values assumed by Dessler (2011), Lindzen and Choi (2011),[1] and Spencer and Braswell (2011), respectively. Here, the ε value is set to zero. Fig. 3a shows generally the upward convex shape with highest correlations and slopes around zero lag. Correlations and slopes are, however, more variable and lower than those in Fig. 2b (the extreme case of $\sigma(F_{rad})/\sigma(F_{non})=0$). Fig. 3b shows similar correlations and slopes at all lags or some distorted shape of the lagged correlation and slope. Fig. 3c shows mostly the distorted shape, which resembles Fig. 2a. All three cases indicate that $\sigma(F_{rad})/\sigma(F_{non})$ smaller than 0.2 can distort the upward convex shape and complicate the estimation of feedback.

Fig. 4 shows more quantitatively the errors in the estimation of feedback with respect to the ratio $\sigma(F_{rad})/\sigma(F_{non})$ as well as $\sigma(\varepsilon)$. The error is calculated by the difference between the regression slope at zero lag and the prescribed true feedback parameter (λ). It should be noted that the bar in Fig. 4 represents only the standard deviation of extensive model runs (100 repetitions), which is much smaller than the actual maximal error. Also, the average of the error should not be emphasized too much since it should approach basically to zero if the error distribution is symmetrical. Results clearly demonstrate that the error increases with the increase in the ratio $\sigma(F_{rad})/\sigma(F_{non})$ for the same λ. The error also significantly increases with the increase in sampling error (ε). More importantly, the error is considerable even for very small $\sigma(F_{rad})/\sigma(F_{non})\sim 0.05$, particularly in the presence of $\sigma(\varepsilon)$ (Fig. 4a). For smaller $\sigma(F_{rad})/\sigma(F_{non})$, the ε value also plays an important role in increasing the error. Comparing Fig. 4a, b, and c, the error increases with the increase in λ if all other factors are equal. Interestingly, the error is slightly biased upward for the system with positive feedback (λ=1 W m^{-2} K^{-1}), whereas more greatly downward for the system with negative feedback (λ=6 W m^{-2} K^{-1}). That is to say, feedbacks (positive or negative) tend to be underestimated, more greatly for negative feedback than for positive feedback.

The above simulations clearly show that non-feedback radiative variations strongly affect the lagged covariance between the two observed quantities. The lag serves to determine whether the observed data favors the estimation of feedback or not. It is therefore essential to consider ΔRs that lead and lag ΔT_ss; only the top of the upward convex shape according to the lag should be identified with feedbacks.

4 Observational assessment of non-feedback variations

Our simple model simulations imply that the slope at zero lag cannot be correctly indicative of the climate feedback in the

[1] Lindzen and Choi (2011) stated that the variances of F_{rad} and F_{non} are 0.7, and 5, respectively. However, they were meant to be standard deviations, i.e., $\sigma(F_{rad})$=0.7, and $\sigma(F_{non})$=5.

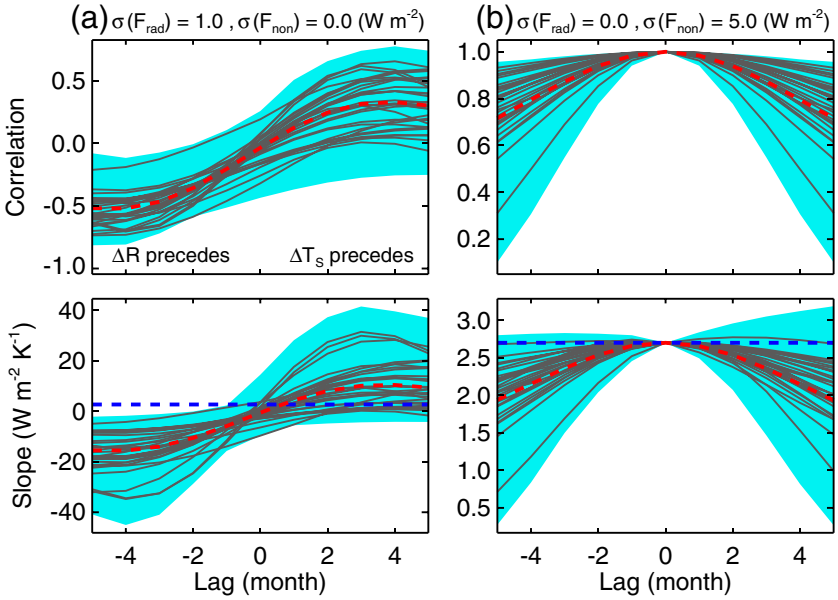

Fig. 2 The lagged linear correlation coefficient and regression slope of ΔR versus ΔT_s from the zero-dimensional energy balance model simulations. The *blue shaded area* indicates the range of the simulated values from 1,000 simulated realizations, and the *red dashed line* indicates their average. The assumed climate feedback 2.7 W m^{-2} K^{-1} is superimposed by the *blue dashed line* in the lagged slope graph. The *thin solid lines* are 30 randomly selected examples. The forcings are purely radiative (**a**) and non-radiative (**b**), respectively

CERES observations if the lagged correlation is distorted according to the lag. This was the case when the temperature change is largely induced by non-feedback radiative variations (or simply noise). To clarify the effect of noise in the currently available data, we attempt to calculate F_{rad} and F_{non}. Here, we obtain these values systematically from the observations in the framework of our simple model. By separating F_{rad} and F_{non} in Eq. 1 into two independent equations, we obtain as follows:

$$F_{rad}(t) = \lambda \cdot \Delta T_s(t) - \Delta R_{TOA}, \tag{3a}$$

$$F_{non}(t) = C_p \left[\frac{d\Delta T_s}{dt}\right] + \Delta R_{TOA} \tag{3b}$$

where ΔR_{TOA} and ΔT_{s} are the same observational data as used in Fig. 1; both are globally averaged monthly anomalous values deseasonalized against the monthly mean for the first 5 years (March 2000–February 2005). Thus, F_{rad} and F_{non} are also anomalies relative to the first 5-year means as they are derived from the anomaly data of ΔR_{TOA} and ΔT_{s}. ΔR_{TOA} is used instead of ΔR for the calculation of F_{rad} and F_{non}, since

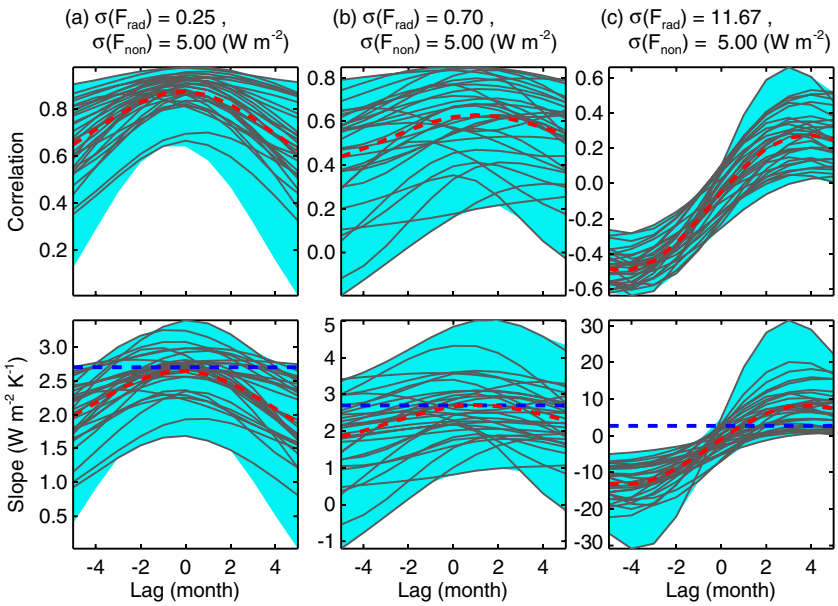

Fig. 3 The lagged linear correlation and regression slope for coexisting radiative and non-radiative forcings with $\sigma(F_{\mathrm{rad}})/\sigma(F_{\mathrm{non}})$=0.05 (**a**), 0.14 (**b**), and 2.33 (**c**)

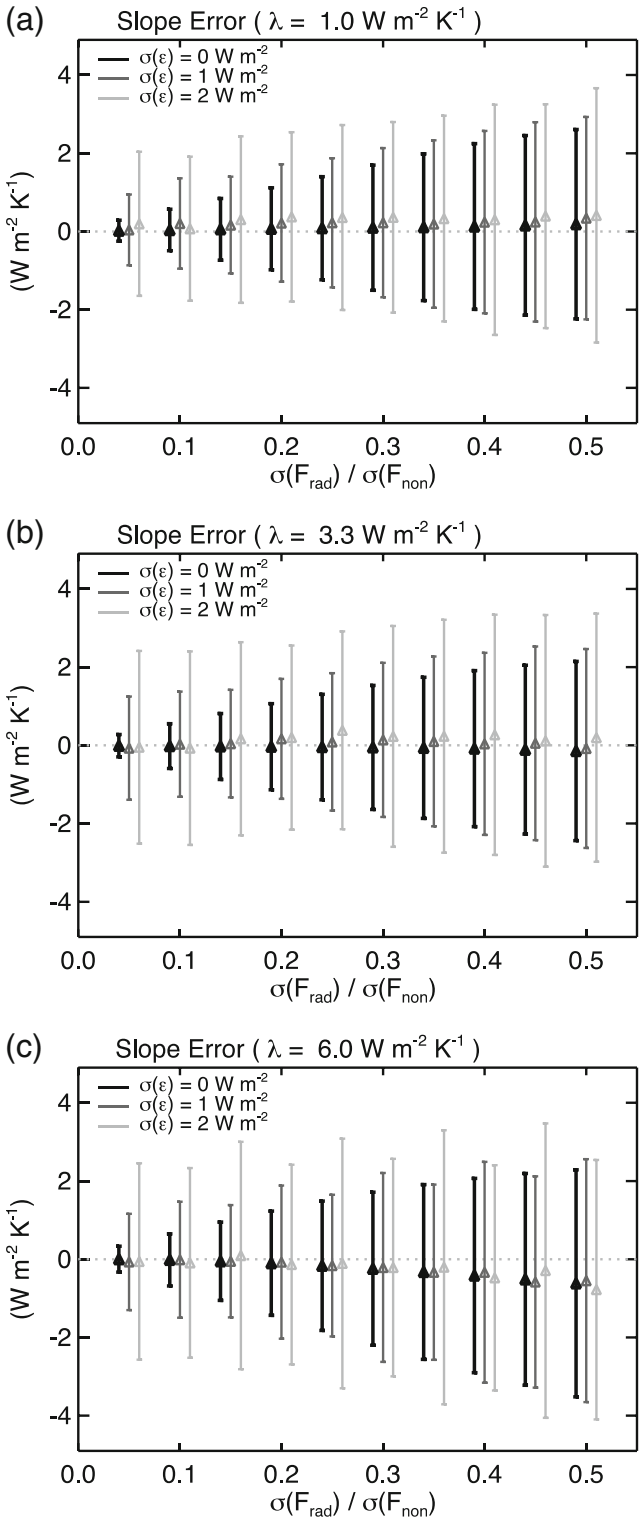

Fig. 4 The mean and standard deviation of the errors in estimated feedback parameter (λ) from 100 simulations of the energy balance model. The abscissa indicates the ratio, $\sigma(F_{rad})/\sigma(F_{non})$. The predescribed feedback parameter is 1.0 W m^{-2} K^{-1} (**a**), 3.3 W m^{-2} K^{-1} (**b**), and 6.0 W m^{-2} K^{-1} (**c**)

ΔR_{TOA} is directly measured. F_{rad} is calculated by Eq. 3a for a specified λ. F_{non} is calculated by Eq. 3b independently of λ.

Because ΔR_{TOA} contributes to the calculation of both F_{rad} and F_{non} in Eq. 3, there is a correlation between F_{rad} and F_{non} that is dependent on λ: r =−0.04 for λ=0 W m^{-2} K^{-1} to −0.19 for λ=8 W m^{-2} K^{-1} when using globally averaged CERES ΔR_{TOA} data (solid line in Fig. 5); the stronger the negative feedback (larger λ), the stronger is the negative correlation between F_{rad} and F_{non}. In addition, in the case of using ΔR_{TOA} averaged over the ocean only (blue dotted line in Fig. 5), F_{rad} and F_{non} have slightly stronger negative correlation (r =−0.11 for λ=0 W m^{-2} K^{-1} to −0.23 for λ=8 W m^{-2} K^{-1}). However, in the case of using ΔR_{TOA} averaged over the land only (red dotted line in Fig. 5), the correlation is similar to or slightly weaker than that for globally averaged ΔR_{TOA}. In order to compare the observationally based estimates with climate models, we also applied Eq. 3 to the Coupled Model Intercomparison Project (CMIP) runs in IPCC AR4 (2007) (Lindzen and Choi 2011); we used λ values that correspond to IPCC AR4 (2007). In terms of correlation between F_{rad} and F_{non}, climate models (plus marks in Fig. 5) have enormously different characteristics from the observation (the solid line in Fig. 5).

As we documented in the previous section, variations of F_{rad} and F_{non} indicate the noise effects on estimating climate feedback. Figure 6 shows the estimated magnitudes of $\sigma(F_{rad})$ and $\sigma(F_{rad})/\sigma(F_{non})$. While not shown explicitly in the figure, $\sigma(F_{non})$ is found to be 5.27 for globally averaged ΔR_{TOA} (5.32 for the ocean-averaged ΔR_{TOA}) in the observation, while CMIP models have a wide range of $\sigma(F_{non})$ (3 to 9 in Table 1). From the observation in Fig. 6a, $\sigma(F_{rad})$ with an increase in λ between 0.7 and 0.9 W m^{-2}. Only a few CMIP models show values comparable to these observational values. Dependence on ΔR_{TOA} should also be mentioned; $\sigma(F_{rad})$ for λ=3.3 W m^{-2} K^{-1} is 0.74 for globally averaged ΔR_{TOA}, 0.80 for the ocean-averaged ΔR_{TOA}, and 1.13 W m^{-2} for the land-averaged ΔR_{TOA}. Thus, land includes larger non-feedback noise than the ocean or the globe. This supports our earlier finding that the estimation of global feedback is more difficult than the estimation of tropical feedback as seen in Fig. 1.

$\sigma(F_{rad})/\sigma(F_{non})$ is calculated to be approximately from 0.13 to 0.18 for the global and ocean ΔR_{TOA} (black dashed and blue dotted lines, respectively), within the possible range of λ in the observations (Fig. 6b). For the land-averaged ΔR_{TOA} (red dotted line), the $\sigma(F_{rad})/\sigma(F_{non})$ value is much larger than that for the global and ocean ΔR_{TOA}. More detailed results on dependence on C_p and λ from the observation are summarized in Table 2. Fig. 6b also shows that $\sigma(F_{rad})/\sigma(F_{non})$ from CMIP models varies from 0.11 to 0.28, for λ around 1 W m^{-2} K^{-1}. This is perhaps the reason why the CMIP models also yield the S-shaped curve in the lagged analyses (Lindzen and Choi 2011). On the other hand, it is possible that the C_p values used here (14 year W m^{-2} K^{-1}) might be too large for the ocean mixed layer of the observed climate or the CMIP models, especially in monthly time scale.

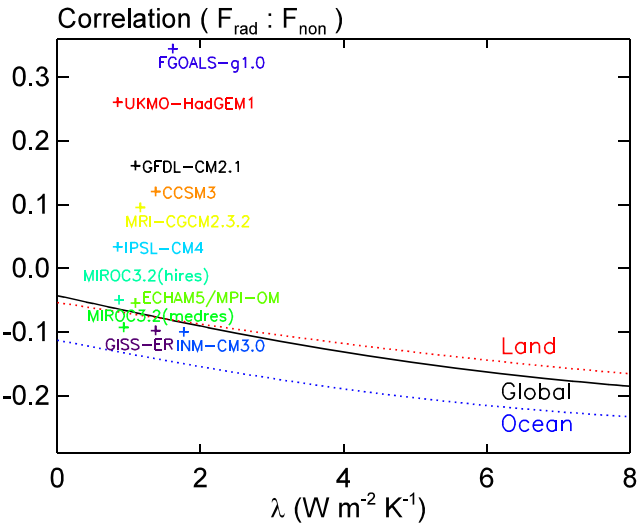

Fig. 5 The correlation coefficient (r) between estimated F_{rad} and F_{non} with respect to feedback parameter λ. From the CERES and SST observations (*solid line* for globally averaged ΔR_{TOA}, *blue dotted line* for the ocean-averaged ΔR_{TOA}, *red dotted line* for the land-averaged ΔR_{TOA}) and from the 11 CMIP climate models (*plus marks*) with the estimated values of λ by CO_2 doubling equilibrium experiments (IPCC 2007)

In our estimations, the dependency of F_{non} on C_p is almost linear, therefore $\sigma(F_{rad})/\sigma(F_{non})$ is almost proportional to C_p^{-1}. For instance, when C_p is set to 10 year W m^{-2} K^{-1}, the values in Fig. 6b increase by a factor of nearly 1.4 (=14/10); $\sigma(F_{rad})/\sigma(F_{non})$ is approximately from 0.19 to 0.22 in the observations and from 0.15 to 0.38 in the CMIP models.

5 Conclusions and discussions

In this study, we have shown that the observational estimation of climate feedback in the $\Delta R-\Delta T_s$ analyses remains very unstable (changes in sign between negative and positive time lags in Fig. 1). Only LW in the tropics (20°S–20°N) shows a highest correlation at zero time lag, allowing reliable estimation of climate feedback. Based on our simple energy balance modeling, the distorted shape (in which a highest correlation does not appear at zero lag) is found to be due to radiative forcings mainly from non-feedback noise, as well as instrumental/sampling errors in the observations. Indeed, variability of radiative forcings relative to that of non-radiative forcings obtained from observations should be large enough to impact the estimation of feedback. The critical level of noise leading to failure of feedback estimation by the simple regression was found to be approximately 0.05.

Current estimates of $\sigma(F_{rad})/\sigma(F_{non})$ (≈0.16–0.20) that are far above the critical level needed to misrepresent feedback indicate that the major climate variations come not only from the ocean heat (mainly in association with natural oscillations like the El Niño Southern Oscillation) but also from non-feedback noise (mainly in association with autonomous cloud

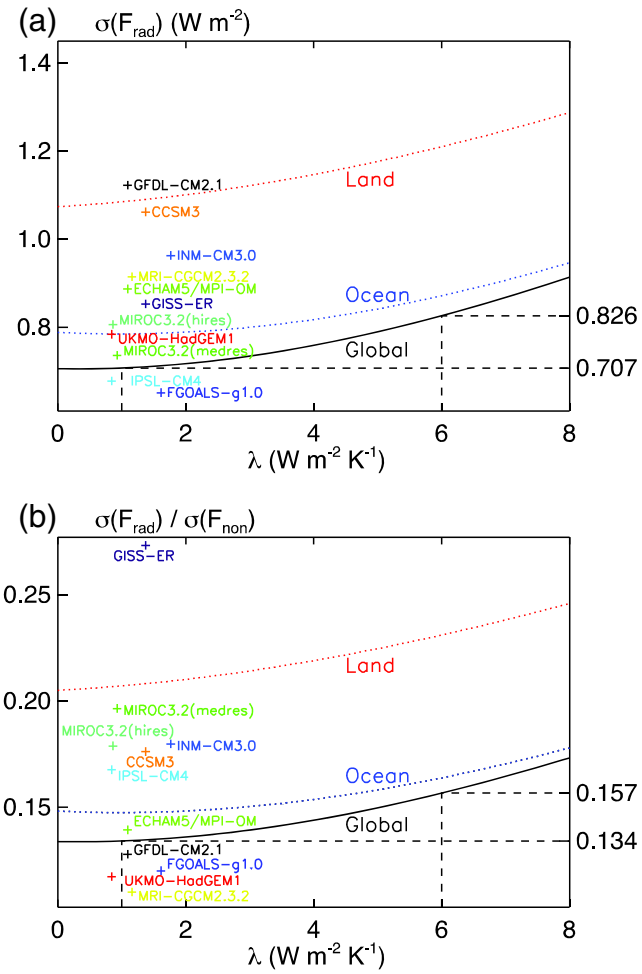

Fig. 6 The correlation coefficient between $\sigma(F_{rad})$ (**a**) and $\sigma(F_{rad})/\sigma(F_{non})$ (**b**) not r. The ratio, $\sigma(F_{rad})/\sigma(F_{non})$ from observations is larger than four models and smaller than six models

changes). While claims exist that $\sigma(F_{rad})/\sigma(F_{non})$ is small enough to secure reliable estimation of feedback from the $\Delta R-\Delta T_s$ analysis, the present result shows that the noise could not be ignored. Rather, the observations as well as various simulations of the simple model strongly support that

Table 1 The estimated $\sigma(F_{non})$ values for 11 CMIP climate models

Models	$\sigma(F_{non})$ (W m^{-2})
GFDL-CM2.1	8.78
GISS-ER	3.12
FGOALS-g1.0	5.42
INM-CM3.0	5.36
IPSL-CM4	4.04
MIROC3.2 (hires)	4.51
MIROC3.2 (medres)	3.75
ECHAM5/MPI-OM	6.36
MRI-CGCM2.3.2	8.31
CCSM3	6.03
UKMO-HadGEM1	6.68

Table 2 The estimated $\sigma(F_{rad})/\sigma(F_{non})$ values associated with different choices for the bulk heat capacity of the Earth's climate system C_p and feedback function λ

Area	C_p	$\sigma(F_{non})$	$\sigma(F_{rad})/\sigma(F_{non})$		
	(yr W m^{-2} K^{-1})	(W m^{-2})	(λ=1.0 W m^{-2} K^{-1})	(λ=3.3 W m^{-2} K^{-1})	(λ=6.0 W m^{-2} K^{-1})
Global	10	3.78	18.7 %	19.6 %	21.9 %
	14	5.27	13.4 %	14.1 %	15.7 %
	21	7.90	9.0 %	9.4 %	10.5 %
	28	10.54	6.7 %	7.0 %	7.8 %
Ocean	10	3.83	20.5 %	21.0 %	22.7 %
	14	5.32	14.7 %	15.1 %	16.4 %
	21	7.95	9.9 %	10.1 %	11.0 %
	28	10.58	7.4 %	7.6 %	8.2 %
Land	10	3.77	28.8 %	29.9 %	32.1 %
	14	5.24	20.7 %	21.5 %	23.1 %
	21	7.85	13.8 %	14.4 %	15.4 %
	28	10.47	10.4 %	10.8 %	11.5 %

Globally averaged, the ocean-averaged, and the land-averaged ΔR values are used

the present level of noise is high enough to prevent reliable estimations of feedback.

A similar study to investigate $\sigma(F_{rad})/\sigma(F_{non})$ was carried out by Dessler (2011), but here, we have to explain why our estimate is much larger than that from Dessler (2011) (~0.05) by clarifying the difference in methodology between our study and his study. This is firstly because the detailed values of ΔR and ΔT_s used in the two studies are different. As we mentioned above, due to many other problems involved in restricting consideration to clouds, this study used total variation in flux, ΔR. Though ΔR contains cloud-induced variation in flux (ΔR_{cloud}) used in Dessler (2011), ΔR is completely different from ΔR_{cloud}. The time variation of ΔT_s in this study is smaller than in Dessler (2011) because of the different SST data sources used. Secondly, Dessler (2011) obtained F_{non} and F_{rad} from incomplete formulas, $F_{non}=C_p\,[d\Delta T_s/dt]$ and $F_{rad}=\Delta R$ (instead of ΔR_{TOA} minus the feedback term); as a result of which, $\sigma(F_{non})$ and $\sigma(F_{rad})$ are much smaller than the results from Eq. 3.

Atmospheric models in which sea surface temperature is prescribed also have cloud variations that change R, but not T_s, in their transient simulations. Thus, their lagged covariances also seem to be distorted by non-feedback variations. Consequently, the similar distorted shape of the lagged covariance in both models and observations cannot guarantee the accuracy of the models' climate feedbacks; rather, they may simply be due to the noise. Under the distorted shape, it is more likely that the noise leads to underestimated positive or negative feedback.

Other than the spurious impact of non-feedback noise on the determination of feedback, an additional problem can arise from the use of regression over the whole record. The problem here stems from the fact that feedbacks introduce temporary imbalances to the radiative budget (over time scales of hours to months), but over longer periods (years to decades depending on climate sensitivity), the system equilibrates so as to eliminate these imbalances (Lindzen and Choi 2009, 2011). Using the whole record acts to distort the feedback estimates by including equilibration in addition to feedback. In the whole record, the increasing radiative forcing such as that due to increasing CO_2 forcing should be considered. If such increasing radiative forcing is added in Eq. 1, it is clearly found that the peak at zero lag in Fig. 2b has been shifted and the linear regression approach fails. This has been already shown in Spencer and Braswell (2010) and Lindzen and Choi (2011) with much stronger statistical significance. Therefore, more accurate estimation of feedback requires the isolation of the specific feedback signals (Lindzen and Choi 2009, 2011; Spencer and Braswell 2010, 2011).

The above concerns suggest that longer data may not be what is crucial to obtain accurate feedbacks because the fundamental limitation is not with the length of data but with the nature of the climate system randomly and radiatively forced by non-feedback noise. Further studies should focus more on isolation of this non-feedback noise, in order to significantly reduce uncertainty in climate feedbacks. Recently, Cho et al. (2012) used clear sky sea surface temperature that may be least affected by non-feedback noise. This study suggested a possibility to successful isolation of non-feedback variations of longwave radiation at least within an active convective cloudy region, the tropical western Pacific. This was actually possible by making use of hourly cloud mask from geostationary satellite observations. Yet, isolation of noise in association with solar reflection remains as a great challenge.

Acknowledgement This study is supported by the Korea Meteorological Administration Research and Development Program under grant CATER 2012–3064 and by the National Research Foundation of Korea (NRF) grant funded by the Korea government (MSIP) (2009-83527).

References

Cho H, Ho CH, Choi YS (2012) The observed variation in cloud-induced longwave radiation in response to sea surface temperature over the Pacific warm pool from MTSAT-1R imagery. Geophys Res Lett 39: L18802

Choi YS, Song HJ (2012) On the numerical integration of a randomly forced system: variation and feedback estimation. Theor Appl Climatol 110:97–101

Choi YS, Lindzen RS, Ho CH, Kim J (2010) Space observations of cold-cloud phase change. Proc Natl Acad Sci U S A 107:11211–11216

Chung ES, Soden BJ, Sohn BJ (2010) Revisiting the determination of climate sensitivity from relationships between surface temperature and radiative fluxes. Geophys Res Lett 37:L10703

Colman R (2003) A comparison of climate feedbacks in general circulation models. Clim Dyn 20:865–873

Dessler AE (2011) Cloud variations and the Earth's energy budget. Geophys Res Lett 38

Forster PM, Gregory JM (2006) The climate sensitivity and its components diagnosed from Earth Radiation Budget data. J Clim 19:39–52

Frankignoul C (1999) A cautionary note on the use of statistical atmospheric models in the middle latitudes: comments on 'decadal variability in the North Pacific as simulated by a hybrid coupled model'. J Clim 12: 1871–1872

Frankignoul C, Czaja A, L'Heveder B (1998) Air–sea feedback in the North Atlantic and surface boundary conditions for ocean models. J Clim 11:2310–2324

Gregory J, Webb M (2008) Tropospheric adjustment induces a cloud component in CO_2 forcing. J Clim 21:58–71

IPCC (Intergovernmental Panel on Climate Change) (2007) Climate change 2007: the physical science basis. Contribution of working group I to the fourth assessment report of the Intergovernmental Panel on Climate Change. Cambridge University Press, Cambridge

Knutti R, Hegerl GC (2008) The equilibrium sensitivity of the Earth's temperature to radiation changes. Nat Geosci 1:735–743

Lin B, Min Q, Sun W, Hu Y, Fan TF (2011) Can climate sensitivity be estimated from short-term relationships of top-of-atmosphere net radiation and surface temperature? J Quant Spectrosc Radiat Transf 112:177–181

Lindzen RS, Choi YS (2009) On the determination of climate feedbacks from ERBE data. Geophys Res Lett 36:L16705

Lindzen RS, Choi YS (2011) On the observational determination of climate sensitivity and its implications. Asia-Pacific J Atmos Sci 47:377–390

Manabe S, Bryan K, Spelman MJ (1990) Transient response of a global ocean–atmosphere model to a doubling of atmospheric carbon dioxide. J Phys Ocean 20:722–749

Murphy DM (2010) Constraining climate sensitivity with linear fits to outgoing radiation. Geophys Res Lett 37:L09704

Roe GH, Baker MB (2007) Why is climate sensitivity so unpredictable? Science 318:629–632

Schwartz ES (2007) Heat capacity, time constant, and sensitivity of Earth's climate system. J Geophys Res 112:D24S05

Soden BJ, Held IM (2006) An assessment of climate feedbacks in coupled ocean–atmosphere models. J Clim 19:3354–3360

Spencer RW, Braswell WD (2010) On the diagnosis of radiative feedback in the presence of unknown radiative forcing. J Geophys Res 115: D16109

Spencer RW, Braswell WD (2011) On the misdiagnosis of surface temperature feedbacks from variations in Earth's radiant energy balance. Remote Sens 3:1603–1613

Trenberth KE, Fasullo JT, O'Dell C, Wong T (2010) Relationships between tropical sea surface temperature and top-of-atmosphere radiation. Geophys Res Lett 37:L03702

Wielicki BA, Barkstrom BR, Baum BA, Charlock TP, Green RN, Kratz DP, Lee RB, Minnis P, Smith GL, Wong T, Young DF, The CERES, Team S (1998) Clouds and the Earth's Radiant Energy System (CERES): algorithm overview. IEEE Trans Geosci Remote Sens 36:1127–1141